The KCNQ/M-current modulates arterial baroreceptor function at the sensory terminal in rats

Cynthia L. Wladyka[1], Bin Feng[2], Patricia A. Glazebrook[1], John H. Schild[2] and Diana L. Kunze[1]

[1]*Rammelkamp Center for Education and Research, MetroHealth Medical Center and Departments of Neurosciences, Case Western Reserve University, Cleveland, OH 44109, USA*
[2]*Department of Biomedical Engineering, Indiana University Purdue University Indianapolis, Indianapolis, IN 46202, USA*

The ion channels responsible for the pattern and frequency of discharge in arterial baroreceptor terminals are, with few exceptions, unknown. In this study we examined the contribution of KCNQ potassium channels that underlie the M-current to the function of the arterial baroreceptors. Labelled aortic baroreceptor neurons, immunohistochemistry and an isolated aortic arch preparation were used to demonstrate the presence and function of KCNQ2, KCNQ3 and KCNQ5 channels in aortic baroreceptors. An activator (retigabine) and an inhibitor (XE991) of the M-current were used to establish a role for these channels in setting the resting membrane potential and in regulating the response to ramp increases in arterial pressure. Retigabine raised the threshold for activation of arterial baroreceptors and shifted the pressure–response curve to higher aortic pressures. XE991, on the other hand, produced an increase in excitability as shown by an increase in discharge at elevated pressures as compared to control. We propose that KCNQ2, KCNQ3 and KCNQ5 channels provide a hyperpolarizing influence to offset the previously described depolarizing influence of the HCN channels in baroreceptor neurons and their terminals.

(Received 21 September 2007; accepted after revision 28 November 2007; first published online 29 November 2007)
Corresponding author D. L. Kunze: Rammelkamp Center for Research and Education R326, MetroHealth Medical Center, 2500 MetroHealth Drive, Cleveland, OH 44109-1998, USA. Email: dkunze@metrohealth.org

Monitoring blood pressure is the key function of a subset of visceral sensory neurons of the nodose ganglia. A select group of nodose neurons, collectively forming the aortic depressor nerve (ADN), project to the aortic arch where they form baroreceptor terminals that respond to the stretch of the arterial wall. It is generally accepted that ion channels, activated by distortion of the sensory terminal, produce a depolarizing receptor potential that initiates action potential discharge proportional to the mechanical distortion at the ending. The information, which is essential for regulation of arterial pressure and heart rate, is relayed through the nodose ganglia to the nucleus of the solitary tract in the brainstem. The pattern of discharge initiated at the terminal region is dependent on the composite of voltage-gated ion channels expressed in the terminal. It is critical that the nerve terminals maintain a stable, negative resting level in the absence of pressure changes to ensure that the sensory information relayed to the central nervous system reflects the distortion of the terminal and not merely intrinsic discharge of the terminal. How this stability is maintained, however, has yet to be fully elucidated.

We have recently demonstrated that KCNQ K^+ channels and the underlying M-current contribute to maintenance of the resting membrane potential in nodose neurons (Wladyka & Kunze, 2006). The aim of our current studies is to determine whether these channels are specifically present in the soma of barosensory neurons and their peripheral sensory terminals. To investigate the functional importance of the channels at the terminal regions, we also recorded unit baroreceptor discharge in the presence of KCNQ inhibitors and activators. We have demonstrated the presence of a retigabine-sensitive M-current under voltage clamp in the soma of labelled aortic baroreceptor neurons. In current-clamp studies, retigabine, a specific M-current activator, hyperpolarized the resting membrane potential whereas XE991, an inhibitor, depolarized the membrane potential. Immunostaining for KCNQ2, KCNQ3 and KCNQ5 was present in the sensory terminals of aortic baroreceptors. In an isolated aortic arch–baroreceptor nerve preparation, slow pressure ramps ($1.3\ \mathrm{mmHg\ s^{-1}}$) were used to generate pressure–discharge curves which were shifted to the right in the presence of retigabine, which is consistent with a hyperpolarization of the resting potential of the sensory terminal membrane. On the other hand, XE991 increased frequency of discharge at the higher pressures, which is consistent with an increase in excitability at the soma.

 DOI: 10.1113/jphysiol.2007.145284

Methods

All animal use protocols were reviewed and approved for ethical practice by the Institutional Animal Care and Use Committees of the authors' respective universities.

Labelling of the ADN

Male Sprague–Dawley rats between 3 and 4 weeks old ($n = 16$) were anaesthetized via intraperitoneal injection with a cocktail of ketamine (25%), xylazine (25%) and acepromazine (50%) at 1.2 ml kg^{-1}. The surgical procedure lasted approximately 10 min, therefore secondary doses of the anaesthetic were not required. The ADN was labelled as previously described (Glazebrook *et al.* 2002). Briefly, all surgical instruments were heat-sterilized for 30 min immediately before surgery. A small incision was made along the trachea at ear level. Muscles and vessels were gently moved aside and the ADN was located adjacent to the left vagus and isolated from surrounding nerves and vessels using a small piece of Parafilm (American National Can) slipped underneath it. A small crystal of DiA (Invitrogen, Molecular Probes) was placed directly on the nerve and held in place by a drop of Kwik-Sil elastimer (World Precision Instruments). The incision was sutured and the animal was given marcaine at 0.1 ml (250 g)$^{-1}$ to alleviate pain during recovery. Animals were monitored postoperatively until they were awake and sternal. Small doses of 0.9% NaCl were given as needed to promote hydration. Animals were closely monitored for 4 days after surgery to allow retrograde transport of the dye up the ADN to the cell body.

Isolation and culture of nodose

Four days after surgery, rats were killed by decapitation and both nodose ganglia (labelled and unlabelled) were extracted, cut into thirds and placed in cold nodose complete medium (NCM; composed of Dulbecco's modified Eagle's medium F-12 (Gibco) supplemented with 5% fetal bovine serum (Cellgro) and 1% penicillin-streptomycin-neomycin antibiotic mixture (PSN; Gibco)). The ganglia were transferred to an enzyme solution containing 1 mg ml^{-1} collagenase type II (Worthington) in Earle's balanced salt solution (Gibco) for 70–80 min at 37°C. The enzyme solution was removed and replaced with NCM containing 1.5 mg ml^{-1} albumin (bovine; Sigma) and the ganglia were dissociated by trituration with fire-polished pipettes. Cells were plated on poly-D-lysine-coated glass coverslips and used within 24 h of plating.

Electrophysiology of baroreceptor neurons

Electrophysiological experiments were performed on fluorescent DiA-labelled nodose neurons at room temperature 22°C, 18–24 h after plating. Using a whole-cell patch configuration under voltage- or current-clamp conditions, data were obtained with an Axopatch-1C patch-clamp apparatus then digitized and analysed using pCLAMP software (Axon Instruments). Electrodes 2–4 MΩ were prepared from 8161 glass (Garner Glass). The extracellular solution for voltage-clamp experiments contained (mM): *N*-methyl-D-glucamine 140 , KCl 5.4, $MgCl_2$ 1, $CaCl_2$ 0.02 and HEPES 10; pH adjusted to 7.3 with HCl. 4-aminopyridine (4-AP; 5 mM) was added to this bath solution in all voltage-clamp experiments to block the K^+ currents that are not pertinent to our studies. *N*-methyl-D-glucamine is not permeable through KCNQ channels (Block & Jones, 1996). The extracellular solution for current-clamp studies contained (mM): NaCl 137, KCl 5.4, $MgCl_2$ 1, $CaCl_2$ 2, glucose 10 and HEPES 10; pH adjusted to 7.3 with NaOH. The pipette solution for voltage and current clamp contained (mM): potassium aspartate 145, HEPES 5, glucose 10, $MgCl_2$ 2, $CaCl_2$ 0.3 and EGTA 2.2; pH adjusted to 7.2 with KOH. Stock solutions of XE991 (Tocris) were made in distilled water and stored at −20°C until diluted in bath solution on the day of the experiment. Retigabine (Valeant Research and Development, Costa Mesa, CA, USA) was directly diluted in bath solution before use in voltage- and current-clamp experiments.

Arch preparation and electrophysiology

Male adult (250–300 g) Sprague–Dawley rats between 8 and 10 weeks old ($n = 4$) were anaesthetized through intraperitoneal injection of a cocktail containing ketamine (87.7%) and xylazine (12.3%) at 0.1 ml (100 g body weight)$^{-1}$. The trachea was cannulated and connected to a small animal ventilator (MODEL 683, Harvard Apparatus) delivering tidal volume of 1.5–2 ml at a rate of 85 min^{-1}. The heart and aortic arch were exposed using a rib spreader along a midsternal incision. The left aortic depressor nerve was identified and separated from the vagus and sympathetic nerves. The aortic arch, right common carotid (RCC), left common carotid (LCC) and left subclavian (LSC) were freed through blunt dissection. These three branching arteries were ligated approximately 5–10 mm away from the junction with the aorta which was also transected from the thoracic trunk. The arch with the ADN was placed in a tissue bath containing warmed mineral oil (37°C). The ascending and descending aorta were cannulated using stainless steel tubing to ensure an anatomically consistent curvilinear flow path. Three branching arteries (RCC, LCC and LSC) were axially stretched to 140–160% of their initial length in order to account for the intrinsic axial tension known to exist within the intact arterial system (Weizsacker *et al.* 1983; Holzapfel *et al.* 1996). The arch

pressure was maintained at 60 mmHg through perfusion at 2–5 ml min^{-1} with Krebs–Henseleit bicarbonate (KHB) buffer which consisted of (mM): NaCl 118, KCl 4.7, $CaCl_2$ 1.25, $MgSO_4$ 1.2, KH_2PO_4 1.2, $NaHCO_3$ 25 and glucose 11.1; equilibrated with 5%CO_2–95% O_2 to give a final pH of 7.35–7.45.

Fascicles of baroreceptor fibres were teased from the ADN trunk using 30 gauge needle tips and mounted onto a bipolar platinum–iridium electrode (FHC Inc., Bowdoin, ME, USA). Dissection continued until one or two identifiable units were obtained. Fibre discharge was amplified using a capacitance-coupled amplifier (Princeton Applied Research, model 113). The nerve recording was digitized in real-time (Model 118, iWorx/CB Sciences, Inc., Dover, NH, USA) at 20 KHz. The spike data were analysed *post hoc* using MATLAB v7.2 (The Mathworks, Inc., Natick, MA, USA) for calculation of instantaneous firing frequency (IFF; the reciprocal of the period between two successive spikes) as a function of intraluminal pressure. From this relationship three distinct measurements were made that captured the essential functional characteristics of each baroreceptor (Andresen & Yang, 1989): (1) the pressure threshold (P_{th}) for baroreceptor nerve discharge calculated as the average pressure over the first 10 spikes; (2) the threshold frequency (F_{th}) of baroreceptor nerve discharge calculated as the average IFF over the 1 s of nerve activity immediately following P_{th}; and (3) the slope (S_{th}) of the IFF–pressure relationship calculated over the first 20–30 mmHg immediately above P_{th}. In order not to evoke the viscoelastic dynamics of the medial smooth muscle, intraluminal pressures were slowly ramped (1.3 mmHg s^{-1}) from 60 to 185 mmHg using a computer-controlled fluid pump (M6, Intelligent Motion Systems). A proportional integral derivative (PID) controller was used to regulate pump pressure, which was continuously monitored using a silicon strain gage pressure transducer (Radnoti Glass Technology).

Isolation and immunohistochemistry of the aortic arch terminals

Sprague–Dawley rats 5–6 weeks old ($n = 14$) were anaesthetized by isofluorane inhalation and subsequently decapitated. The region of the aortic arch containing the innervation by the ADN was isolated and cut lengthwise along the bottom so that the arch could be opened and laid out flat with the inner vessel wall facing up. The muscle was peeled away, leaving only the adventitia containing the nerve terminals. The tissue was prepared for immunohistochemistry as previously described (Doan *et al.* 2004). Each arch was labelled with one KCNQ marker and one nerve marker. Commercial primary antibodies used were goat polyclonal anti-peripherin (Santa Cruz C-19 sc7604, 1 : 300), mouse monoclonal anti-myelin basic protein (Chemicon, MAB 381, 1 : 500), mouse monoclonal anti-KCNQ2 (Neuromab, clone N26A/23, 1 : 200), rabbit polyclonal anti-KCNQ3 (Alomone, APC-051, 1 : 200), rabbit polyclonal anti-KCNQ5 (ABR, PA1–941, 1 : 500), anti-α3Na/KATPase (Santa Cruz, sc-16052, 1:50), mouse monoclonal anti-neurofilament (NF) 68 (Novacastra, NR4, 1:100), mouse monoclonal anti-NF 160 (Sigma, NN18, 1:00), mouse monoclonal anti-NF 200 (Sigma N52, 1:100).

Imaging was performed using the Leica Microsystem SP2 Confocal microscope. Sequential serial stacks at the appropriate wavelength were collected for reconstruction of the nerve terminals using Autoquant software (MediaCybernetics, Silver Spring, MD, USA).

Statistical analysis

Experimental data are presented as means ± S.E.M. A two-tailed Student's *t* test was used to assess statistical significance, which required a P value of 0.05.

Results

KCNQ/M-current identified in ADN soma

By labelling the ADN with DiA and allowing retrograde transport to the cell body, we were able to specifically study the electrophysiological properties of the subset of nodose neurons that project to the aortic arch. Figure 1 shows recordings from a representative fluorescence-labelled cell. Figure 1*A–C* illustrates the currents evoked by the voltage protocol (shown above Fig. 1*C*) in the presence of bath solution (Fig. 1*A*), 10 μM retigabine (Fig. 1*B*), and washout (Fig. 1*C*). The retigabine-sensitive current in Fig. 1*D* was obtained by subtracting that obtained in Fig. 1*A* from that in Fig. 1*B*, and represents the current increased by this compound. The current exhibits the characteristic slow activation of M-current, as well as saturation at higher potentials. Using a single exponential fit, we found this current to have an activation time constant of 213 ± 31 ms at −20 mV ($n = 8$). An example of the fit at −20 mV, as well as at −30 mV, is shown above Fig. 1*D* (black line), overlaid on the original trace (grey). Figure 1*E* shows the current–voltage relationship of normalized current from eight cells for bath solution alone and with retigabine. It is evident that retigabine caused a leftward shift in this curve, as compared to the control curve, and significantly increased current activation ($P < 0.0001$ at −20 mV, $n = 8$) with changes occurring in a range as negative as −60 to −50 mV.

We performed similar voltage-clamp experiments on labelled cells in the presence of the KCNQ-inhibitor, XE991 (data not shown). By subtracting current recordings in the presence and absence of XE991, we were able to isolate the current sensitive to this drug and examine

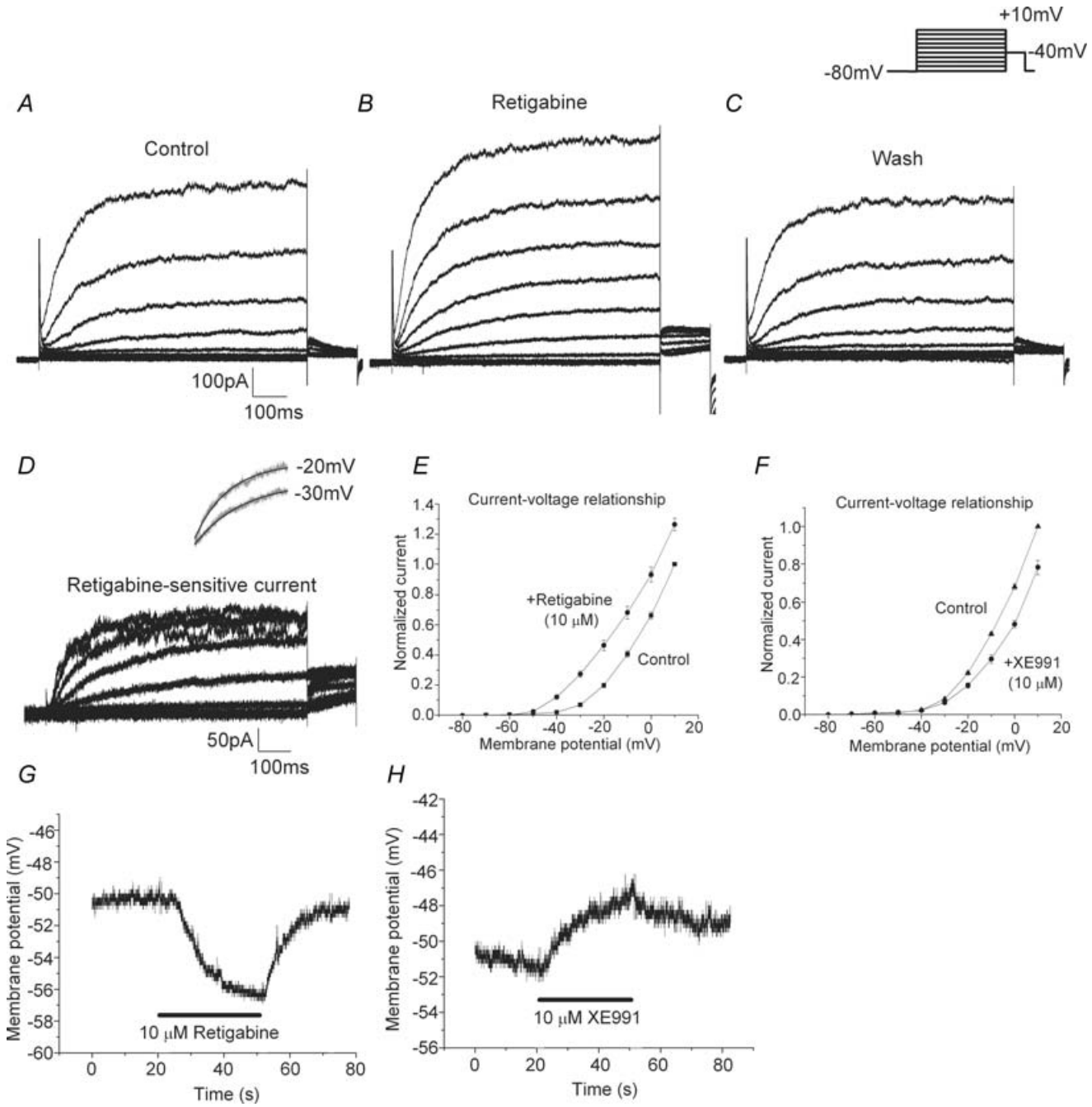

Figure 1. Effects of retigabine and XE991 on baroreceptor neuron soma
Experimental data illustrating current recorded in baroreceptor neurons elicited by the protocol shown in the inset (800 ms pulse from a holding potential of −80 mV to a step voltage between −80 and +10 mV in 10 mV increments and finally back to −40 mV for 150 ms) that was applied in the absence (*A*), presence (*B*) and washout (*C*) of 10 μM retigabine. The retigabine-sensitive current (*D*) was obtained by subtracting the current shown in *A* from that in *B*. Activation time constants were determined from mono-exponential fits of the incremental pulses from −80 mV to the step voltages. The inset above *D* shows the mono-exponential fit (black line) overlaid on the original traces (grey) for steps to −30 and −20 mV. The current–voltage relationships (*E* and *F*) were plotted as the voltage step *versus* the normalized current at 800 ms for the data in the presence of retigabine (●, in *E*) and XE991 (●, in *F*), and their respective control currents (■, in *E* and ▲ in *F*). Current-clamp recordings of the effect of 10 μM retigabine (*G*) and 10 μM XE991 (*H*) on representative cells with resting membrane potentials of −51 mV. In *G*, retigabine was applied between 20 and 50 s whereas in *H*, XE991 was applied between 20 and 50 s.

its activation properties. In particular, we found it to have a single activation time constant of 211 ± 23 ms at -20 mV ($n = 7$), a value nearly identical to that seen for the retigabine-sensitive current. Figure 1*F* shows a current–voltage plot with the normalized current from seven cells for control and in the presence of XE991. It is clear that XE991 reduced current activation ($P < 0.02$ at -20 mV, $n = 7$).

Figure 1*G* and *H* illustrates current-clamp recordings of the resting membrane potential of labelled cells in the presence of retigabine and XE991, respectively. The membrane potential of the cell in Fig. 1*G* was resting near -50 mV and the addition of retigabine caused a rapid hyperpolarization to approximately -56 mV. This effect was readily reversible within 10 s of washout. Similar significant effects were seen in a total of eight cells with an average hyperpolarization of 7.5 ± 1.1 mV (range 2–11 mV, $P < 0.0002$, $n = 8$). Finally, as seen in Fig. 1*H*, we examined the effects of XE991 on resting membrane potential and observed a depolarization in the presence of this drug. The effect was not notably reversible upon washing, as also noted in our previous studies with XE991. For eight cells, a significant depolarization of 5.6 ± 1.4 mV (range 2–14 mV) was seen ($P < 0.005$, $n = 8$), with effects seen on cells at a resting potential as negative at -56 mV.

These data support the presence of M-current in the subset of nodose neurons projecting to the aortic arch.

Distribution of KCNQ2, KCNQ3 and KCNQ5 on baroreceptor terminals

We previously demonstrated the presence of variable amounts of immunoreactivity for KCNQ2, KCNQ3 and KCNQ5 in the soma of nodose neurons (Wladyka & Kunze, 2006). Here we examined the baroreceptor terminals for the presence of KCNQ immunoreactivity. Immunoreactivity against all three KCNQ proteins was located in the baroreceptor terminals which generally fall into three categories: receptors of large diameter myelinated fibres with branching fibres forming plate-like endings connected by narrower regions (Fig. 3); smaller myelinated fibres that terminate abruptly often with an enlargement at the end (Fig. 2); and unmyelinated fibres. We localized the nerve fibres as follows. A cocktail of anti-neurofilament (NF200, NF160, NF68) antibodies was used to label the large- and medium-diameter fibres and anti-peripherin antibody was used to label medium- to smaller-diameter fibres. The anti-α3Na/KATPase antibody labels myelinated fibres and is particularly useful because it extends into the plate-like regions of the terminal endings, whereas the other two neuronal markers are seldom found there. Examples of the distribution of anti-KCNQ2 in small- and medium-sized fibres are shown in Fig. 2. The distribution of KCNQ3 and KCNQ5 in the terminals of large myelinated fibres is illustrated in Fig. 3. Anti-KCNQ3 was also abundant in the non-neuronal cells surrounding the terminal ending whereas anti-KCNQ5 was only present in a subpopulation of these cells.

Pharmacological effects of retigabine and XE991 applied at the terminals

To investigate whether the KCNQ proteins in the baroreceptor terminals were actually forming functional channels, we utilized an intact arch–nerve preparation to simulate the *in vivo* conditions. Each fibre recording consisted of four successive trials using the same pressure ramp protocol (1.3 mmHg s^{-1}) from 60 to 185 mmHg. Because the exchange of fluids through the arch muscle layer is a limiting factor, each trial was carried out after at least 30 min perfusion through the arch at 60 mmHg, which ensured that the drug application (retigabine and XE991 (both 10 μM) via the perfusate) and the washout achieved a steady-state level of effectiveness. All control recordings were obtained from myelinated fibres and exhibited three robust characteristic features: (1) an abrupt onset of nerve discharge at P_{th}, followed by (2) a relatively

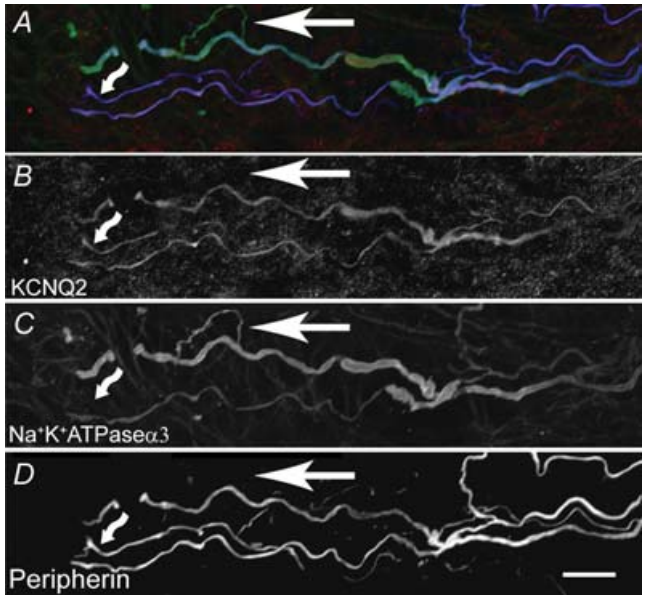

Figure 2. KCNQ2 expression in baroreceptor terminals in the aortic arch
A, is an overlay of a three-dimensional reconstruction image of baroreceptor nerve terminals taken from confocal sequential three-channel series. *B–D*, single channel views of *A*. Two different antibodies, anti-peripherin (blue) and anti-α3Na/KATPase (green) were used to identify nerve fibres as neither labels all nerve fibres. KCNQ2 (red) was present in most but not all nerve fibres as indicated a fibre (arrow) that is not labelled with either peripherin or KCNQ2. The KCNQ2 is also present in a fine fibre that co-labels with peripherin, but not α3Na/KATPase and is most probably an unmyelinated fibre ('wavy' arrow). Scale bar, 15 μm.

linear range of pressure encoding that (3) asymptotically approached a maximum IFF (Fig. 4*A*). The values for these parameters were compared for each fibre in both control and the test solution containing the drug (Andresen & Yang, 1989). Following 30 min of perfusion with KHB and the selective KCNQ agonist retigabine, a repeat pressure ramp showed a shift in the pressure–discharge curve to higher pressures. P_{th} increased from 80 to 99 mmHg and IFF (at 150 ± 1 mmHg) markedly decreased from 35 to 25 Hz (Fig. 4*B*) such that the discharge failed to reach saturation at 185 mmHg (highest pressure tested). The average values for four fibres are given in Fig. 4. We noted a significant increase in average P_{th} and decrease of average IFF at 150 ± 1 mmHg. There were also small changes in S_{th} and F_{th}; however, these differences failed to achieve statistical significance. Figure 4*C* illustrates a control level after 30 min of perfusion with KHB, followed by the selective KCNQ antagonist XE991, leading to a dramatic increase in the average IFF at 150 ± 1 mmHg from 38 to 44 Hz (Fig. 4*D*). For three fibres in the presence of XE991, a significant increase of was average IFF was observed at 150 ± 1 mmHg, as well a significant increase in average measures of P_{th} and S_{th}, but the change in average F_{th} was not statistically significant ($P > 0.05$).

Discussion

In this study, we provide evidence of M-current and KCNQ proteins in the specific subset of neurons of the nodose ganglia that innervate the aortic arch, as well as in the baroreceptor terminals themselves. We know from previous work (Wladyka & Kunze, 2006) that the nodose population, as a whole, expresses KCNQ2, KCNQ3 and KCNQ5, the molecular correlates of neuronal M-current. However, these authors noted variability in the level of expression, which led to the question of the contribution of the M-current to a specific subset of nodose neurons, the aortic arterial baroreceptors. By labelling the ADN and allowing retrograde transport to the soma, we were able to focus our current study solely on the neurons with projections to the aortic arch, to determine whether this particular group of neurons contains functional amounts of M-current. Using the well known M-current agonist retigabine and antagonist XE991, we were able to confirm the presence of current with M-like characteristics in these neurons.

This current exhibited the slow activation and lack of inactivation that is a hallmark of M-current seen by us (Wladyka & Kunze, 2006) as well as by many others (Brown & Adams, 1980; Adams *et al.* 1982; Tinel *et al.* 2000; Gamper *et al.* 2003). Although this current was small

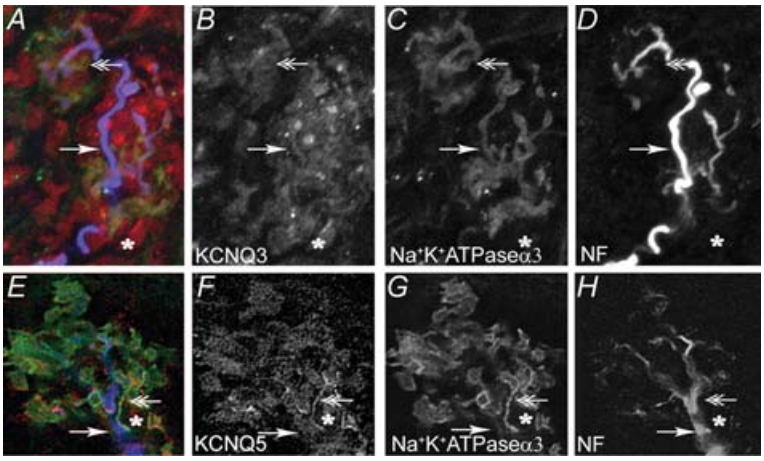

Figure 3. Confocal three-dimensional reconstruction of a series of optical slices of baroreceptor large-diameter myelinated fibres
An anti-neurofilament cocktail (blue) was used to label the major fibre branches and anti-α3Na/KATPase (green) labelled the major branches as well as the plate-like structures that make up the final terminal region. *A–D*, overlay of anti-rabbit KCNQ3 antibody (red) with anti-neurofilament cocktail and anti-α3Na/KATPase. The single arrowhead indicates colabelling of the major fibre branch with all three antibodies. KCNQ3 also labels many of the non-neuronal accessory cells that closely surround the nerve terminal and that are labelled by neither neuronal marker; an example is indicated by the asterisk in each of *A–D*. The double arrowhead indicates an example of the co-labelling by KCNQ3 antibody with the α3Na/KATPase in one of the plate-like structures of the terminal. *E–H*, overlay of anti-KCNQ5 antibody with anti-neurofilament cocktail and anti-α3Na/KATPase is shown in a major fibre branch (arrow). The asterisks show a cell located in close proximity to the terminal stained with KCNQ5 antibody (red) but not with the neuronal markers. A small fibre labels with anti-KCNQ5 and anti-α3Na/KATPase but not anti-NF (double arrowhead). Scale bars, 10 μm.

(Fig. 1*D*), we also showed that it was activated at negative potentials in the range of the resting potential (Fig. 1*F* and *G*), indicating its role in maintaining stability at the level of the cell body.

However, critical events occur at the level of the baroreceptor terminal in the aortic arch where the sensory terminals are activated by stretch of the terminal region. Our immunohistochemistry data illustrate clear expression of KCNQ2, KCNQ3 and KCNQ5 proteins in the baroreceptor endings. The data from our whole-arch preparation support a functional role for these potassium channel subunits at the baroreceptor terminals.

Functional role of M-current at the baroreceptor terminals

Although it has not been directly measured, it is presumed that stretch of the arterial baroreceptor terminal leads to the opening of a strain-sensitive cation channel, depolarization of the terminal ending and initiation of action potential discharge in the afferent nerve fibre. An increase in baroreceptor discharge leads to a reflex decrease in sympathetic outflow to the heart and vessels and an increase in vagal cardiac outflow. The characteristics of the discharge are largely governed by the integrated ionic current arising from multiple ion channels present in the terminal region, most of which have yet to be identified. We have identified members of the HCN family that can provide a depolarizing inward current at the baroreceptor terminals at near resting membrane potentials (Doan *et al.* 2004). From the results of the present study we have also identified members of the KCNQ potassium channel family that would provide an opposing hyperpolarizing force near the resting membrane potential. Retigabine, an M-current activator, increases the pressure threshold for spike generation by an average of 19.0 ± 5 mmHg ($n = 4$). An increase in threshold would be expected given the hyperpolarizing effect retigabine was shown to have upon the resting membrane potential of baroreceptor neurons, leading to

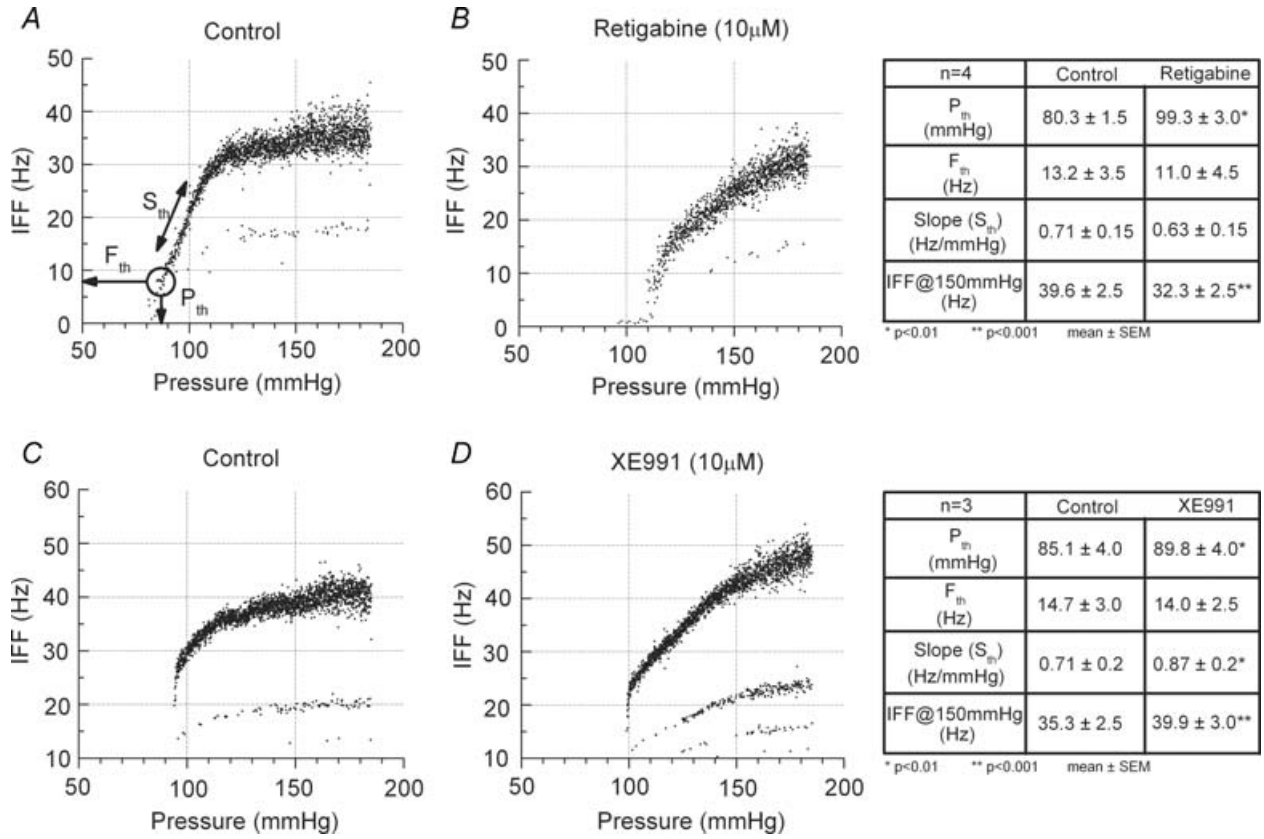

Figure 4. Functional impact of KCNQ agonist and antagonist on baroreceptor discharge
From a conditioning pressure of 60 mmHg, intraluminal pressure was ramped (1.3 mmHg s^{-1}) from 60 to 185 mmHg under the following successive conditions: control perfusion of KHB. Measures P_{th}, F_{th} and S_{th} are explained in the Methods and are shown in the tables to the right of each corresponding pair (control and drug) (*A*); following 30 min perfusion of KHB + 10 μM retigabine (*B*); following 30 min perfusion of KHB as washout (*C*); following 30 min perfusion of KHB + 10 μM XE991 (*D*). The paired control and retigabine recordings (*A* and *B*) and the paired control and XE991 recordings (*C* and *D*) were from two different baroreceptor fibres.

increased stability and decreased excitability. Retigabine also had the effect of shifting the discharge–pressure curve to higher pressures, decreasing the overall IFF at a specific pressure. Without compensation, this would lead to a shift to higher pressures in the reflex control of blood pressure and heart rate. It is interesting that the M-current inhibitor XE991 also had the effect of raising the threshold, although much less than retigabine. This may reflect the role of a decrease in sodium channel availability with the XE991-induced depolarization of the resting potential. At higher pressures (150 mmHg), there is an increase in nerve firing frequency, which is similar to its effect when recording in current-clamp mode at the soma (Wladyka & Kunze, 2006). The pattern of discharge presumably reflects the state of other channels when activated from the depolarized potential. Additionally, it is known that the M-current activator retigabine and the M-current inhibitor XE991 used in this study can potentially affect the other KCNQ family members, KCNQ1 and KCNQ4 (Wang *et al.* 2000; Schroder *et al.* 2001; Sogaard *et al.* 2001; Tatulian *et al.* 2001). However, we know of no evidence for expression of either of these two subunits in visceral sensory neurons.

Monitoring and faithfully encoding changes in blood pressure is a critical function, and demonstration of a functional role for KCNQ/M-current in the neuron soma as well as in the baroreceptor terminals of the aortic arch underscores the importance of maintaining stability in this highly regulated system.

References

Adams PR, Brown DA & Constanti A (1982). M-currents and other potassium currents in bullfrog sympathetic neurons. *J Physiol* **330**, 537–572.

Andresen MC & Yang M (1989). Arterial baroreceptor resetting: contributions of chronic and acute processes. *Clin Exp Pharmacol Physiol Suppl* **15**, 19–30.

Block BM & Jones SW (1996). Ion permeation and block of M-type and delayed rectifier potassium channels. *J Gen Physiol* **107**, 473–488.

Brown DA & Adams PR (1980). Muscarinic suppression of a novel voltage-sensitive K^+ current in a vertebrate neurone. *Nature* **283**, 673–676.

Doan T, Stephans K, Glazebrook PA, Ramirez A, Andresen MC & Kunze DL (2004). Differential distribution and function of hyperpolarization-activated channels (I_H) in sensory neurons and mechanosensitive fibers. *J Neurosci* **24**, 3335–3343.

Gamper N, Stockand JD & Shapiro MS (2003). Subunit-specific modulation of KCNQ potassium channels by src tyrosine kinases. *J Neurosci* **23**, 84–95.

Glazebrook PA, Ramirez A, Schild JH, Shieh C-C, Doan T, Wible BA & Kunze DL (2002). Potassium channels, Kv1.1, Kv1.2 and Kv1.6, influence excitability of rat visceral sensory neurons. *J Physiol* **541**, 467–482.

Holzapfel GA, Eberlein R, Wriggers P & Weizsacker HW (1996). A new axisymmetrical membrane element for anisotropic, finite strain analysis of arteries. *Comm Num Meth Eng* **12**, 507–517.

Schroder RL, Jespersen T, Christophersen P, Strobaek D, Jensen BS & Olesen SP (2001). KCNQ4 channel activation by BMS-204352 and retigabine. *Neuropharmacology* **40**, 888–898.

Sogaard R, Ljungstrom T, Pedersen KA, Olesen SP & Jensen BS (2001). KCNQ4 channels expressed in mammalian cells: functional characteristics and pharmacology. *Am J Physiol Cell Physiol* **280**, C859–C866.

Tatulian L, Delmas P, Abogadie FC & Brown DA (2001). Activation of expressed KCNQ potassium currents and native neuronal M-type potassium currents by the anti-convulsant drug retigabine. *J Neurosci* **21**, 5535–5545.

Tinel N, Diochot S, Lauritzen I, Barhanin J, Lazdunski M & Borsotto M (2000). M-type KCNQ2-KCNQ3 potassium channels are modulated by the KCNE2 subunit. *FEBS Lett* **480**, 137–141.

Wang HS, Brown BS, McKinnon D & Cohen IS (2000). Molecular basis for differential sensitivity of KCNQ and IKs channels to the cognitive enhancer XE991. *Mol Pharmacol* **57**, 1218–1223.

Weizsacker HW, Lambert H & Pascale K (1983). Analysis of the passive mechanical properties of rat carotid arteries. *J Biomech* **16**, 703–715.

Wladyka CL & Kunze DL (2006). KCNQ/M currents contribute to the resting membrane potential in rat nodose sensory neurons. *J Physiol* **575**, 175–189.

Acknowledgements

The authors would like to thank Valeant Pharmaceuticals (Costa Mesa, CA, USA) for their generous gift of retigabine. This work was supported by National Institutes of Health grants HL061436 to D.L.K. and HL072012 to J.H.S.